Korean Journal of Remote Sensing, Vol.19, No.3, 2003, pp.255~261

A Study on Aerial Triangulation from Multi-Sensor Imagery

Young-Ran Lee*, Ayman Habib, Kyung-Ok Kim*****

Image/System Devision, SaTReCi Co.*

Department of Geomatics Engineering, University of Calgary**

GIS Research Team, Spatial and Visual Information Technology Center

Electronic and Telecommunications Research Institute***

Abstract : Recently, the enormous increase in the volume of remotely sensed data is being acquired by an ever-growing number of earth observation satellites. The combining of diversely sourced imagery together is an important requirement in many applications such as data fusion, city modeling and object recognition. Aerial triangulation is a procedure to reconstruct object space from imagery. However, since the different kinds of imagery have their own sensor model, characteristics, and resolution, the previous approach in aerial triangulation (or georeferencing) is performed on a sensor model separately. This study evaluated the advantages of aerial triangulation of large number of images from multi-sensors simultaneously. The incorporated multi-sensors are frame, push broom, and whisky broom cameras. The limits and problems of push-broom or whisky broom sensor models can be compensated by combined triangulation with other sensors The reconstructed object space from multi-sensor triangulation is more accurate than that from a single model. Experiments conducted in this study show the more accurately reconstructed object space from multi-sensor triangulation.

Key Words : Multi-Sensor Model, Aerial Triangulation, Bundle Adjustment.

1. Introduction

The recent development of new sensors has created a need for data processing techniques that can fuse observations from a variety of different sensors. Recent research in multi-sensor integration and fusion systems has proved the benefits and robust characteristics of such approaches for a wide variety of applications. The interdisciplinary nature of data fusion makes it a very powerful technique with applications to industrial inspection, remote sensing and military surveillance, robotics, medical diagnosis and even financial market analysis. One of the key benefits is the enhancement of sensor data through integration to improve the certainty and quality of the information provided (Pohl and van Genderen, 1998). The exploitation of satellite images and more generally of observations of the Earth and our environment is presently one of the most productive in data fusion. Multi-sensor data fusion is an evolving technology concerned with the problem of how to combine data and information from multiple sensors in order to achieve improved accuracies and better

Received 5 March 2003; Accepted 20 May 2003.

inference about the environment than could be achieved by the use of a single sensor alone. Since, the set of sensors for Earth observation is extremely various, the spectrum of their characteristics is very large, with respect to spatial and temporal scales, spatial and temporal sampling and means of acquisition. Such diversity is a tremendous source of practical problems, whose resolutions lie upon a good understanding and modeling of more fundamental questions (Csatho and Schenk, 1998). The integration of multi-temporal and multi-sensor remote sensing data and other relevant data layers demand appropriate georeferencing methods. Only if such methods are available, the new information resulting from the combination of the source datasets can be optimally utilized by the various users. Only, after applying data is georeferenced in the same coordinates, new information can be gained from the complementary information content of the multiple data sources. It is recognized that the data have to undergo a respective pre-processing, including geometric as well as radiometric procedures. These pre-processing steps are in general very critical points for operational data fusion applications and, therefore, cannot be viewed independently from the applied data fusion methods.

This paper is related to the geometric pre-processing of multi-temporal and multi-sensor images, so that a subsequent pixel-level image fusion is possible. Moreover, any method in georeferencing that reduce the number of ground control points needed to achieve a desired level of accuracy would greatly reduce the cost of a project. Fusion of the multiple sources of imagery would benefit in the triangulation and data capture environments. Performing simultaneous adjustment of all image types has got the benefit of taking advantages of the different imagining systems' best characteristics. However, all these benefits come with only if the mathematical and physical models of the different systems are considered. (Ackerman, 1995).

In this research, we will present the generalized mathematical model for block adjustment of multi-sensor systems in section 2. Section 3 will show the experimental result of applied model. Finally, conclusion and future works are followed in section 4.

2. Mathematical Model

1) Generalized Collinearity Equation for Multisensor Model

Habib and Beshah(1998) proposed a generalized mathematical model to integrate frame, pushbroom, three-line and panoramic sensor model. The panoramic linear array scanner is composed of a number of CCD line sensors mounted in the focal plane. The sensor in the focal plane is parallel to the flight direction and successive area coverage is obtained by rotating the telescope containing the imaging sensor in the cross track direction. Because panoramic sensor model is the most generalized model among the different sensor models, the collinearity equation is extended to form light ray in panoramic line scanner with rotation angle and image motion compensation (Eq. 1).

$$
\begin{aligned}
x_t &= x_p + imc(t) - f\frac{r_{11t}(X_G - X_{Ot}) + r_{12t}(Y_G - Y_{Ot}) + r_{13t}(Z_G - Z_{Ot})}{r_{31t}(X_G - X_{Ot}) + r_{32t}(Y_G - Y_{Ot}) + r_{33t}(Z_G - Z_{Ot})} \\
x_t &= x_p - f\frac{r_{21t}(X_G - X_{Ot}) + r_{22t}(Y_G - Y_{Ot}) + r_{23t}(Z_G - Z_{Ot})}{r_{31t}(X_G - X_{Ot}) + r_{32t}(Y_G - Y_{Ot}) + r_{33t}(Z_G - Z_{Ot})}
\end{aligned}
\tag{1}
$$

where

t	image epoch for each scan line
x_t, y_t	image coordinate measurement with respect to the telescope coordinate system
X_G, Y_G, Z_G	object coordinates of a point
x_p, y_p, f	calibrated principal point position and focal length of the camera
$r_{11t}, r_{12t}, \cdots r_{33t}$	elements of the rotation matrix $R_t = R(a_t)R(\omega_t, \phi_t, \kappa_t)$ at time t

a_t	the swing angle at time t
$imc(t)$	image motion compensation at time t
X_{Ot}, Y_{Ot}, Z_{Ot}	coordinate of the perspective center at time t

Three line scanner is another type of line scanners which has triple CCD lines on the same focal plane. The output images consist of triple coverages on the ground by forward, nadir, and backward-looking scanners. Three line scanner is also can use the same generalized collinearity equations (Eq. 1) with the modification that a_t and $imc(t)$ are set to zero. Pushbroom scanner is a specialized case of three-line scanner which has one nadir looking scanners. It can be treated as same as the three-line scanners.

An image taken by a frame camera has a perspective or central projection. The extended collinearity equation also works with the modification that a_t and $imc(t)$ are set to zero and the EOP are not dependent on time since it has only one perspective center.

2) Applied Model for Block Adjustment

A scene captured by a linear array scanner (panoramic scanner, three line and pushbroom) is composed of scan lines, each having a set of unknown exterior orientation parameters (EOP). That is each row has its own EOP. This results in a large number of unknown parameters. There are two ways to reduce the number of involved parameters to avoid singularities in solution process. A very simple way is the use of a polynomial modeling the system's trajectory, which determines the change in the EOP with time. However, the system trajectory might be too rough to be modeled by a polynomial. In addition, it is difficult to incorporate additional information for GPS/INS observations. Another approach to reduce the number of EOP is using the concept of orientation images (OI). Orientation images are usually designed at equal intervals along the system's trajectory. In this research, OI is used to compute the sensor's trajectory because it is much easier to incorporate GPS/INS observations directly, which is available in auxiliary data of imagery. The GPS/INS observation is included in bundle adjustment by the relationship between the observed GPS coordinates and the unknown ground coordinates of the perspective center (Eq. 2).

$$\begin{bmatrix} X_{GPS} \\ Y_{GPS} \\ Z_{GPS} \end{bmatrix} = \begin{bmatrix} X_{Ot} \\ Y_{Ot} \\ Z_{Ot} \end{bmatrix} + R(\omega_t, \phi_t, \kappa_t) \begin{bmatrix} dx \\ dy \\ dz \end{bmatrix} + \begin{bmatrix} ex_{GPS} \\ ex_{GPS} \\ ex_{GPS} \end{bmatrix}$$

$$\text{where} \begin{bmatrix} ex_{GPS} \\ ex_{GPS} \\ ex_{GPS} \end{bmatrix} \cdots (0, \sum_{GPS}) \qquad (2)$$

Similar to the GPS, the computed attitude from INS can be included to the extended bundle adjustment directly (Eq. 3).

$$\begin{bmatrix} \omega_t \\ \phi_t \\ \kappa_t \end{bmatrix}_{INS} = \begin{bmatrix} \omega_t \\ \phi_t \\ \kappa_t \end{bmatrix} + \begin{bmatrix} e\omega \\ e\phi \\ e\kappa \end{bmatrix} \text{ where} \begin{bmatrix} e\omega \\ e\phi \\ e\kappa \end{bmatrix} \cdots (0, \sum_{INS}) \qquad (3)$$

The exterior orientation parameters of a scan line capture at time t are expressed in terms of the exterior orientation parameter associated with neighboring orientation images. General or Lagrangian polynomials that express the EOP as function of time can be applied as the interpolation function between Orientation Images. The image coordinates are considered as observations for a least-square adjustment together with other additional observations: control points, GPS/INS (if available), and any other information about the remaining parameters. The determination can be accomplished using a photogrammetric bundle adjustment. Hence, the image coordinate measurements can be expressed as a function of the unknown parameters (a, imc, IOP, GP, EOP_i, ⋯, EOP_n)of the adjustment, where IOP is the interior orientation parameters, $EOP_{i..n}$ are the exterior orientation parameters of involved orientation image ($1 \sim n$) and GP is the ground control points.

3. Experiments

An extended bundle adjustment program (MSAT: Multi-Sensor Aerial Triangulation) was developed using Visual C++ (Habib, and Beshah, 1998). In this experiments MSAT is used for aerial triangulation of multi-sensor imagery captured by pushbroom scanners and whiskbroom scanners in a simultaneous adjustment. Whiskbroom scanners for LANDSAT-7 can be treated as another specialized scanner type of the generalized panoramic scanners. In case of IKONOS sensor, there are many unknown sensor parameters (especially interior parameters). In the experiments, IKONOS sensor is modeled as same as a general pushbroom sensor, and the unknown sensor parameters are assumed in default values of general pushbroom sensor such as $x_p = 0$, $y_p = 0$ and $f = 10m$. Moreover, in order to converge into a solution during a block adjustment, initial values for unknown parameters are approximated in simple plane projection equation by using control points in object and image spaces. The dataset used in the experiments of this research is shown in Table 1.

The same ground coverage (Daejon/Korea) is selected for multiple images of multi-sensors. The ground truth of GCPs is measured by using GPS instruments with the accuracy of cm level. If the following parameters are considered, the balance of block adjustment is computed as follows.

- Number of images from multi-sensors (M), Number of ground control points (n), Number of tie points (p)
- Number of unknowns is $M \times 6 \times OI$ (Orientation images) $+ p \times 3$ (X, Y, Z in ground coordinates),
- Number of observations is $(p + n) \times 2$ (x, y in image coordinates) $\times M + n \times 3$ (X, Y, Z in ground coordinates).

Table 1. Experiment data sets[1].

Sensor type	Satellite name	Ground resolution
Whiskbroom	LANDSAT 7 (PAN)	15m
Pushbroom	KOMPSAT-1 (PAN)	6m
Pushbroom	SPOT-1 (PAN)	10m
Pushbroom	IKONOS	1m

1 All datasets are provided by ETRI

The most difficult process for the block adjustment of multi-sensor aerial triangulation is the preparing of observations from multiple images with different resolution. The ground control points measured in high-resolution imagery are hard to measure in low-resolution imagery. Moreover, the control points from imagery of low resolution cannot be used in high-resolution imagery since the points are invisible. Resampling high-resolution images into low-resolution will help to measure tie points to overcome the difference of visibility of images. Hence, careful selection of control points must be followed in preparing of observation process. The subpart of test image set from multi-sensors is shown in Fig. 1 with original resolution. After resampling of high-resolution images, control points in high-resolution images can be found more easily in low-resolution images. In this case, the measured accuracy of control points in low-resolution images is not a problem because the error boundary of the measured accuracy will be less than one pixel of the low-resolution image. If control points (tie points) are measured and matched in the resampled image in low resolution, then the points should be propagated into original resolution. Several researches are presented methods to measure control points automatically. The methods use optical flow idea, gray value information content and their local wavelet transform modulus maxima, and centers of gravity of the edges (Fonseca, *et al.*, 1999 and Fonseca and Costa, 1997). However, since measurement errors in image space will propagate directly to the reconstructed object space, careful selection of control points must be followed in preparing of observation process. In this research, the control points are extracted by using an interesting operator and identified in semi-automatic mode. Since tie points are initially extracted by using an

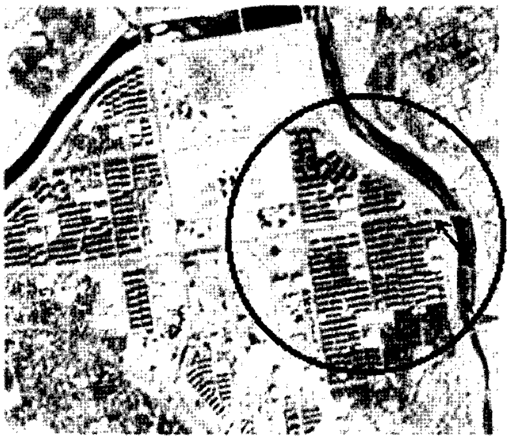

(a) LANDSAT/PAN (15m)

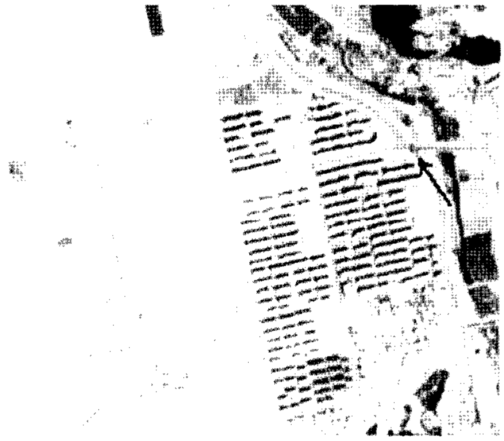

(b) SPOT/PAN(10m) ©SPOT/CNES

(c) KOMPSAT-1/EOC(6m)

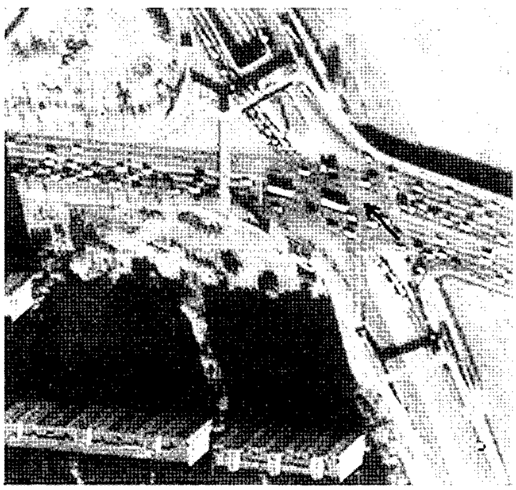

(d) IKONOS/PAN(1m) ©2001 Space Imaging Inc.

Fig. 1. Preparation control points in multi-images.

interesting operator, the points are uniformly distributed in overall image space. If it is possible, the used control points are tried to be located at each image corner and center position.

The accuracy of this experiment is presented with RMS errors of test points after the bundle adjustment. In the first experiment (Table 2) the bundle adjustment is performed separately in an independent sensor model in which the accuracy of image coordinate measurement is a half pixel (σ = 0.5 pixel). As you can see, the RMS values of test points in each sensor model are estimated in sub-pixel accuracy based on the image resolution. In next experiment (Table 3) different combination of sensors are used in block adjustment. Comparing the RMS values in case 4 in Table 2 and case 4 in Table 3 shows that there is a improvement in the accuracy due to the addition of the push-broom image in a whiskbroom image. The RMS values of the whiskbroom sensor are reduced than that of a single sensor adjustment. In other words, the weak geometry of the whiskbroom sensor in across track can be compensated with the geometry of pushbroom sensors. Moreover, the number of GCPs was

Table 2. Bundle adjustment with a sensor[1].

Case No	Description	RMS X (m)	RMS Y(m)	RMS Z(m)
1	Pushbroom (SPOT-1)	6.7	9.9	19.4
2	Pushbroom (KOMPSAT-1)	5.1	5.9	18.6
3	Pushbroom (IKONOS)	1.1	1.7	2.5
4	Whiskbroom (LANDSAT-7)	12.9	14.8	26.7

1.Each bundle adjustment in Table 2 is performed with 15GCPs and 10 test points.

Table 3. Bundle adjustment with different combination of images with different resolutions[2].

Case No	Description	RMS X (m)	RMS Y(m)	RMS Z(m)
1	Pushbroom (SPOT-1 + KOMPSAT-1)	5.7	6.2	9.9
2	Pushbroom (KOMPSAT-1+ IKONOS)	3.3	4.9	6.9
3	Pushbroom sensors (SPOT + KOMPSAT + IKONOS)	1.8	2.1	3.1
4	Pushbroom and Whiskbroom (SPOT + LANDSAT-7)	7.5	11.2	19.9

2. Each bundle adjustment in Table 3 is performed with 5 GCPs, 10 tie points, 10 test points

also decreased with better accuracy. In case 1, 2, and 3 of Table 3, the bundle adjustment is performed in the same pushbroom sensors with images of different resolution. The RMS values of low-resolution imagery are reduced by adding high-resolution images. Moreover, we observed in Table 3 that the varying resolution with the different sensors has minor effect on the output result. The reconstructed object space of multi-sensor images is more accurate than that of single sensor by adding high-resolution images. However, we should note that high-resolution image could be affected by the relatively inaccurate image point measurements of low-resolution images. Therefore, the multi-sensor adjustment can be applied in order to increase the accuracy of available many low-resolution images, decrease the number of control points and provide efficient block adjustment process by adding high-resolution images.

4. Conclusions

Recently, the enormous volume of remotely sensed data is being acquired by an ever-growing number of earth observation satellites. The combining of diversely sourced imagery together demands a generalized model to integrate different types of sensor models in georeferencing of imagery. The ability of combining imagery with different perspective geometry will enable us to utilize all the information available in different imagery.

The result presented in section 3 show that equivalent accuracy could be achieved by using control points or having different sensor images in a simultaneous multi-sensor adjustment. The combination of different sensors has practical benefits when it is too costly or impossible to survey control points or incorporable control points are already available in the adjustment. The improvement by adding more imagery results in the reduction of the number of control points. Moreover, the variation in the resolution of involved imagery had little impact on the accuracy in the object space. For the future work the image point selection and transfer form multi-sensor imagery should be addressed. In addition, the integration of optical as well as non-optical sensor system such as LIDAR and SAR could be considered.

Successful incorporation of these sensors will help to reduce the cost of mapping systems.

References

Ackermann, F., 1995. Sensor and Data Integration - The New Challenge, *Proceeding ISPRS Workshop Integrated Sensor Orientation*, September 1995, Barcelona, pp. 2-10.

Csatho, B. and T. Schenk, 1998. Multisensor Data Fusion for Automatic Scene Interpolation, *International Archives of Photogrammetry and Remote Sensing*, XXXII(7), Budapest, pp. 336-341.

Fonseca, L. M. G., G. Hewer, C. Kenny, and B.S. Manjunath, 1999. Registration and Fusion of Multispectral Images Using a New Control Point Assessment Method Derived from Optical Flow Ideas, *Proceeding SPIE*, 3717, pp. 104-111.

Fonseca, L. M. G. and M. H. M. Costa, 1997. Automatic Registration of Satellite images, *Proceedings, Los Alamitos:IEEE Computer society*, pp. 219-226

Habib, A. and B. T. Beshah, 1997. Modeling Panoramic Linear Array Scanner, *Departmental Report 443*, Civil and Environmental Engineering and Geodetic Science, The Ohio State University, Columbus, Ohio.

Habib, A. and B. T. Beshah, 1998. Multi-sensor Aerial Triangulation, *ISPRS Commission III Symposium* in Columbus, Ohio, July.

Heipke, C., W. Kornus, and A. Pfannenstein, 1996. The Evaluation of MEOSS Airborne 3-line Scanner Imagery-Processing Chain and Results, *Photogrammetric and Remote Sensing*, 62(3): 293-299.

Pohl, C. and J. L. van Genderen, 1998. Multisensor Image Fusion in Remote Sensing: Concepts, Methods, and Application, *International Journal of Remote Sensing*, 19(5): 823-854.